Complex Difference Analysis Provides Insight into Internal Organ of Corti Motion

[1]Lauren Chiriboga, [2]C. Elliott Strimbu, [1,2]Elizabeth S. Olson

[1] Department of Biomedical Engineering Columbia University, New York City, NY

[2] Department of Otolaryngology-Head & Neck Surgery, Columbia University, New York City, NY

Corresponding author email: lauren.chiriboga@columbia.edu

S47

Introduction

Optical coherence tomography (OCT) has been applied to cochlear mechanics to measure motion at multiple intra-organ of Corti (OC) locations simultaneously. Motion measurements are made at individual locations along the OCT's optical axis, but the motion at each location should not be analyzed in a vacuum. Large displacements of one structure could obstruct the underlying motion of other structures if those other structures have much smaller displacements. An example of where this could occur is observing outer hair cell (OHC) or reticular lamina (RL) motion in the context of basilar membrane (BM) motion.

To account for this, we take the complex difference between the motion of a structure (OHC/DC junction or RL region) and BM motion *[1]*. We perform this analysis on data collected from guinea pig (GP). In instances of a large BM motion, the complex difference highlights the underlying structure motion.

Methods

Consider a simplified motion profile of the BM ($\vec{X}_{BM}$) and an internal OC structure ($\vec{X}_{int}$) described by the equations:

$$\vec{X}_{BM} = X_{BM} * e^{i\varphi}$$
$$\vec{X}_{int} = X_{int} * e^{i\theta_{int}}$$

where X_{BM}, X_{int} are the amplitudes of BM and an internal structure motion respectively and φ, θ are the corresponding phases.

When performing OCT vibrometry with a transverse optical view, we consider the transverse BM motion as the basis on which the internal structures sit. Therefore, the motion of an internal structure as observed from the OCT can be understood as the "measured" motion.

$$\vec{X}_{meas} = \vec{X}_{int} + \vec{X}_{BM}$$
$$= X_{meas} * e^{i\theta_{meas}}$$

The two motions sum to contribute to the measured motion, resulting in either constructive or destructive interference, depending on the relative phases.

$$\vec{X}_{meas} = X_{int} * e^{i\theta_{int}} + X_{BM} * e^{i\varphi_{BM}}$$

In instances where the BM motion is much greater than the internal motion, the measured motion of the internal structure appears to be moving like the BM despite the presence of internal motion.

To extract the internal motion, we subtract the BM motion from the measured motion in a complex difference.

$$\vec{X}_{int} = \vec{X}_{meas} - \vec{X}_{BM}$$

This analysis allows for visualization of a structure's internal motion despite much larger BM motion. Alternatively, when BM motion and internal motion are comparable, this analysis shows how they sum, resulting in the structure's measured motion.

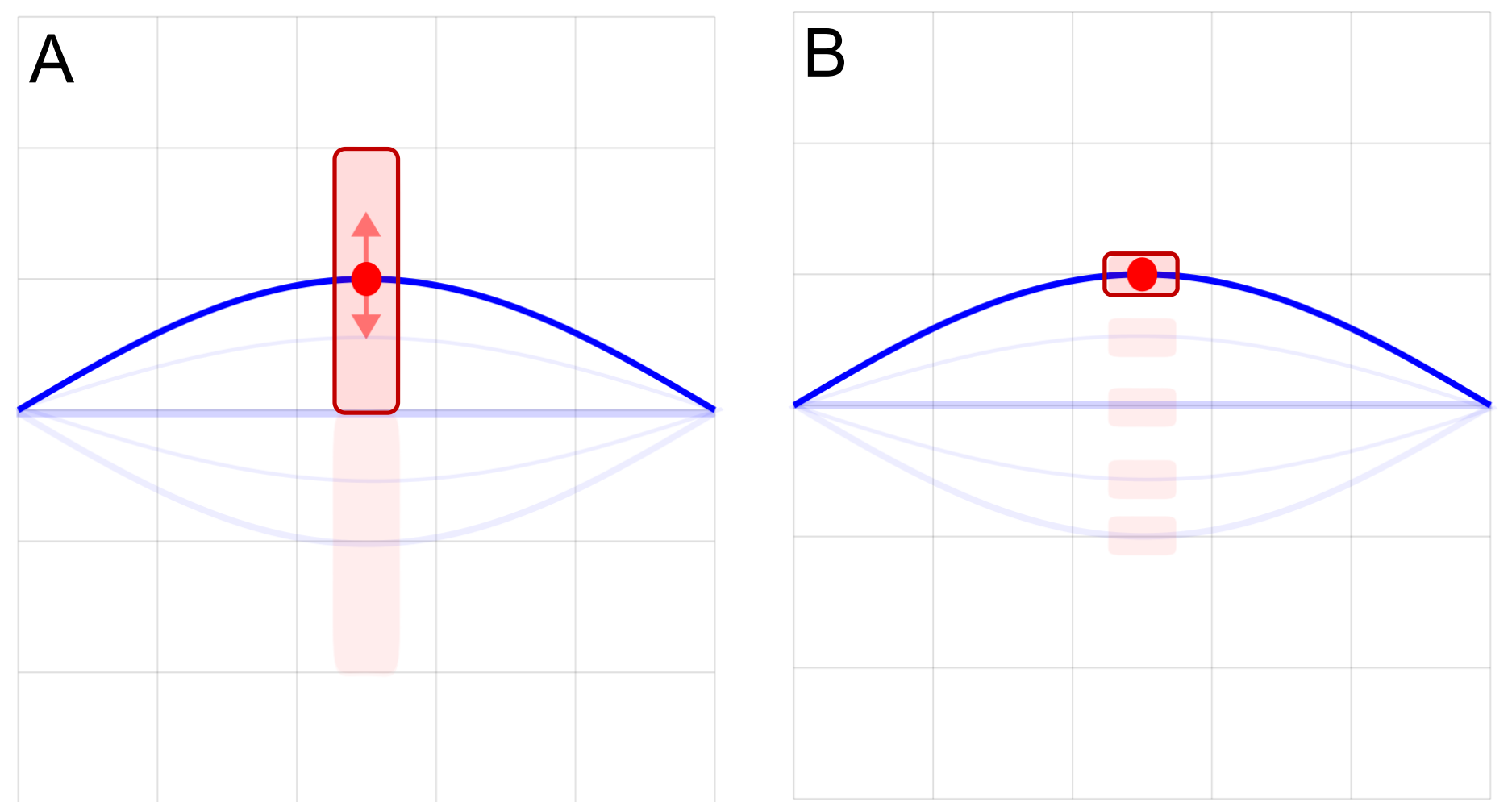

Figure 1: Simplified example of a red ball attached to a blue string, both oscillating. The red shaded regions indicate the possible positions of the ball based on its amplitude and the string's position at a given time. (A) When the amplitudes of the ball and the string are comparable, the ball's motion is easily distinguishable from the string's motion. (B) When the ball's amplitude is much smaller than that of the string, the ball appears to move with the string, despite having its own oscillation.

Experimental Methods

- 1300 nm spectral domain OCT was used for imaging and vibrometry, as described previously *[2-3]*
- Multi-tone Zwuis stimuli were used, containing 35 stimulus frequencies between 5-40 kHz *[4]*
- Motion measurements and imaging were primarily transverse, conducted through the round window (RW) followed by a cochleostomy in the first turn
- Cochlear condition was monitored by DPOAE measurements before and after cochleostomy at 50 and 70-dB sound pressure level (SPL)

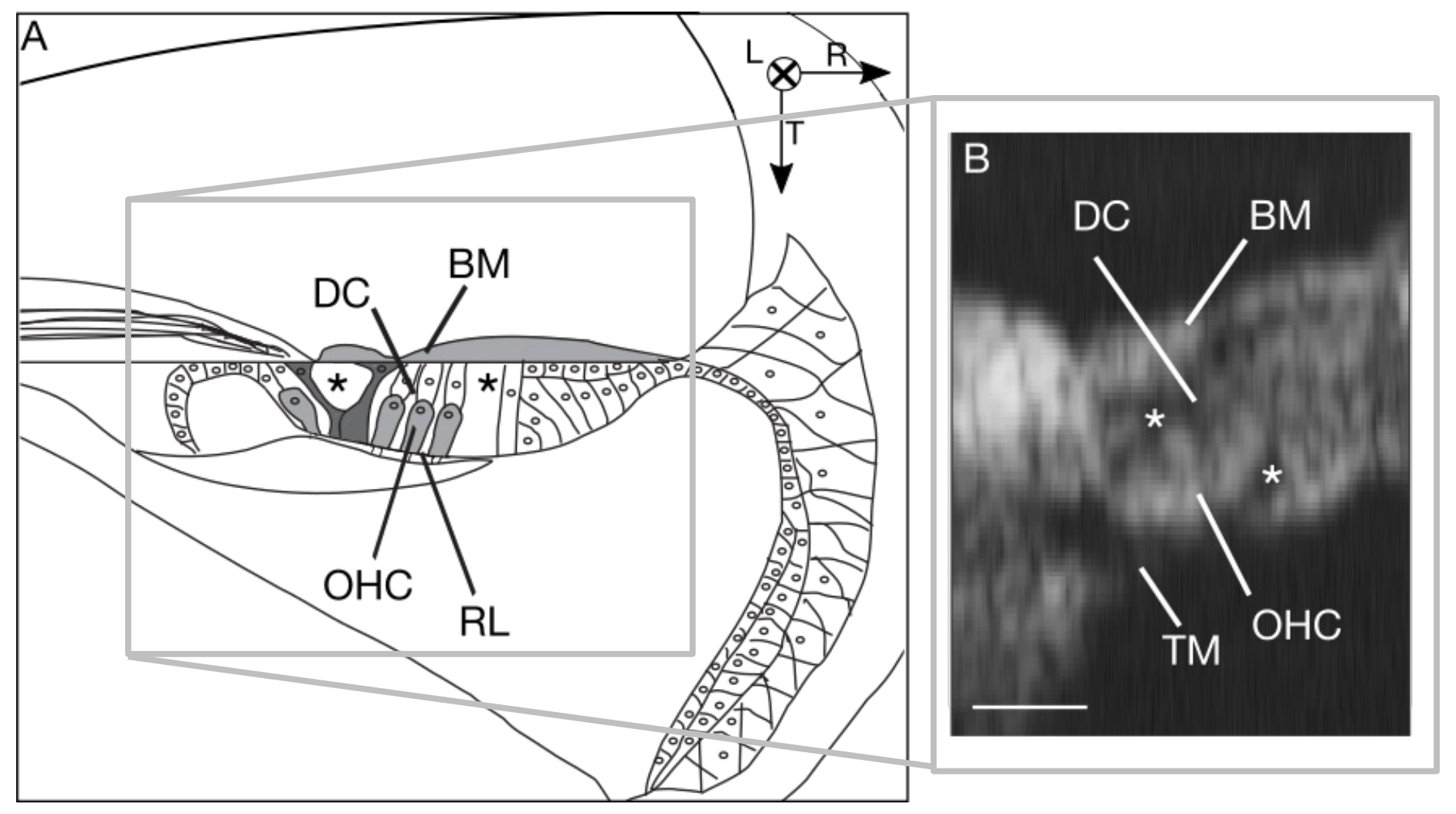

Figure 2: (A) Simplified rendering of a radial-transverse cross-section of the organ of Corti in the cochlear base. Structures of interest are the Basilar Membrane (BM), Tectorial Membrane (TM), outer hair cells (OHCs), reticular lamina (RL), stereocilia, scala media (SM), scala tympani (ST). (B) OCT Bscan of the radial-transverse cross-section with some structures of interest identified.

Data

GP 86 Run 47

- 34 kHz BF measured through RW
- Internal structure of interest: OHC apex/RL region
- Slight sub-BF nonlinearity
- Internal structure phase fan at low frequencies

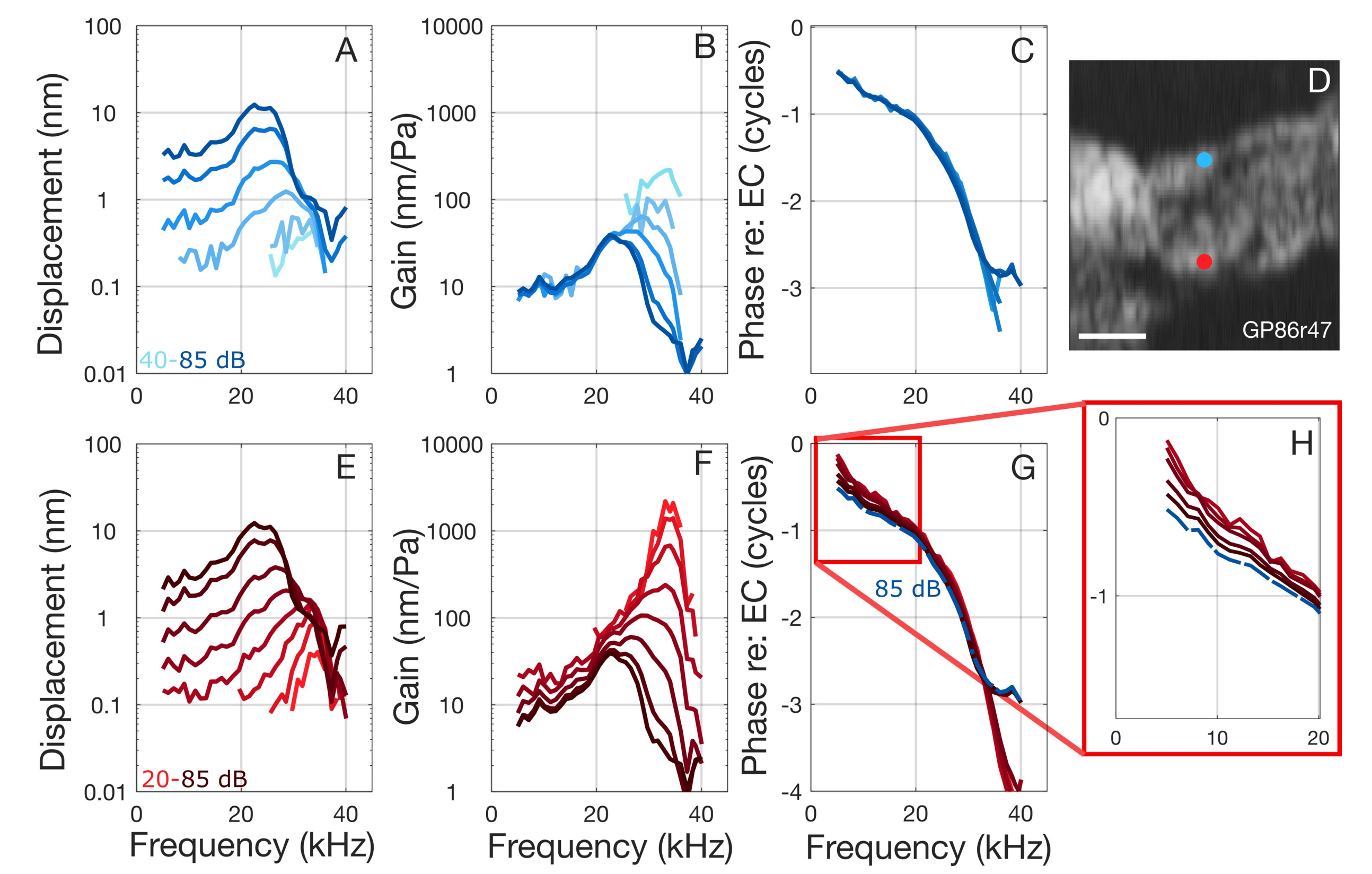

Figure 3: GP86 run 47. (A) BM displacement. (B) BM displacement normalized by ear canal (EC) pressure. (C) BM phases re: EC. (D) Bscan highlighting the BM (blue) and internal structure (red). Scale bar = 50 µm. (E) Internal structure displacement. (F) Internal structure displacement normalized by EC pressure. (G) Internal structure phase re: EC. Also includes BM phase in response to 85 dB SPL for comparison. (H) Internal structure phase zoomed in at low frequencies. The internal structure phase deviates from in phase with BM as sound pressure level decreases.

GP 96 Run 91

- 26 kHz BF measured through cochleostomy
- Internal structure of interest: central OHC body
- Sub-BF nonlinearity – broader tuning
- Internal structure phase shift - meets BM phase at high SPL

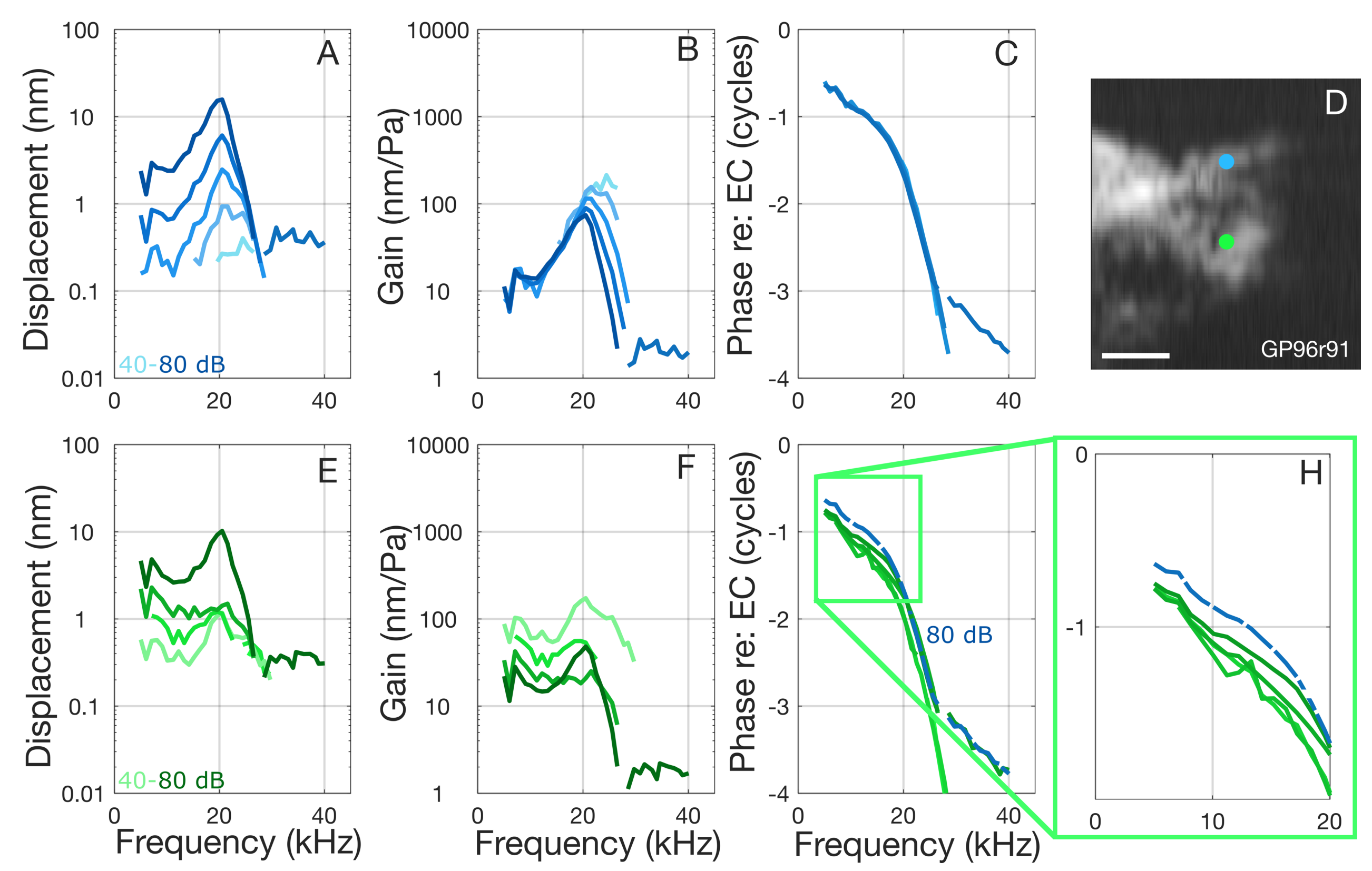

Figure 4: GP96 run 91. (A) BM displacement. (B) BM displacement normalized by EC pressure. (C) BM phases re: EC. (D) Bscan highlighting the BM (blue) and internal structure (green). Scale bar = 50 µm. (E) Internal structure displacement. (F) Internal structure displacement normalized by EC pressure. (G) Internal structure phase re: EC. Also includes BM phase in response to 80 dB SPL for comparison. (H) Internal structure phase zoomed in at low frequencies. At low sound pressure levels, the internal structure phase lags the BM around ¼ cycle. However, at higher SPLs, the internal structure phase approaches BM around BF.

Complex Difference Analysis

BM and Internal Motion Comparisons

1. Comparable magnitudes, in phase
- Measured motion is also in phase and the measured magnitude is BM magnitude + internal magnitude
- Often found at low SPLs near BF

2. Comparable magnitudes, out of phase
- BM and internal motion are approx. ½ cycle out of phase
- Measured motion magnitude appears small
- Measured phase shifts from in phase with internal to in phase with BM near peak

3. BM motion > internal motion
- Very small contributions from internal motion
- Measured motion is approx. BM motion
- Often happens at high SPLs and/or near BF

4. Internal motion > BM motion
- Very small contributions from BM motion
- Measured motion is approx. internal motion
- Occurs at low frequencies

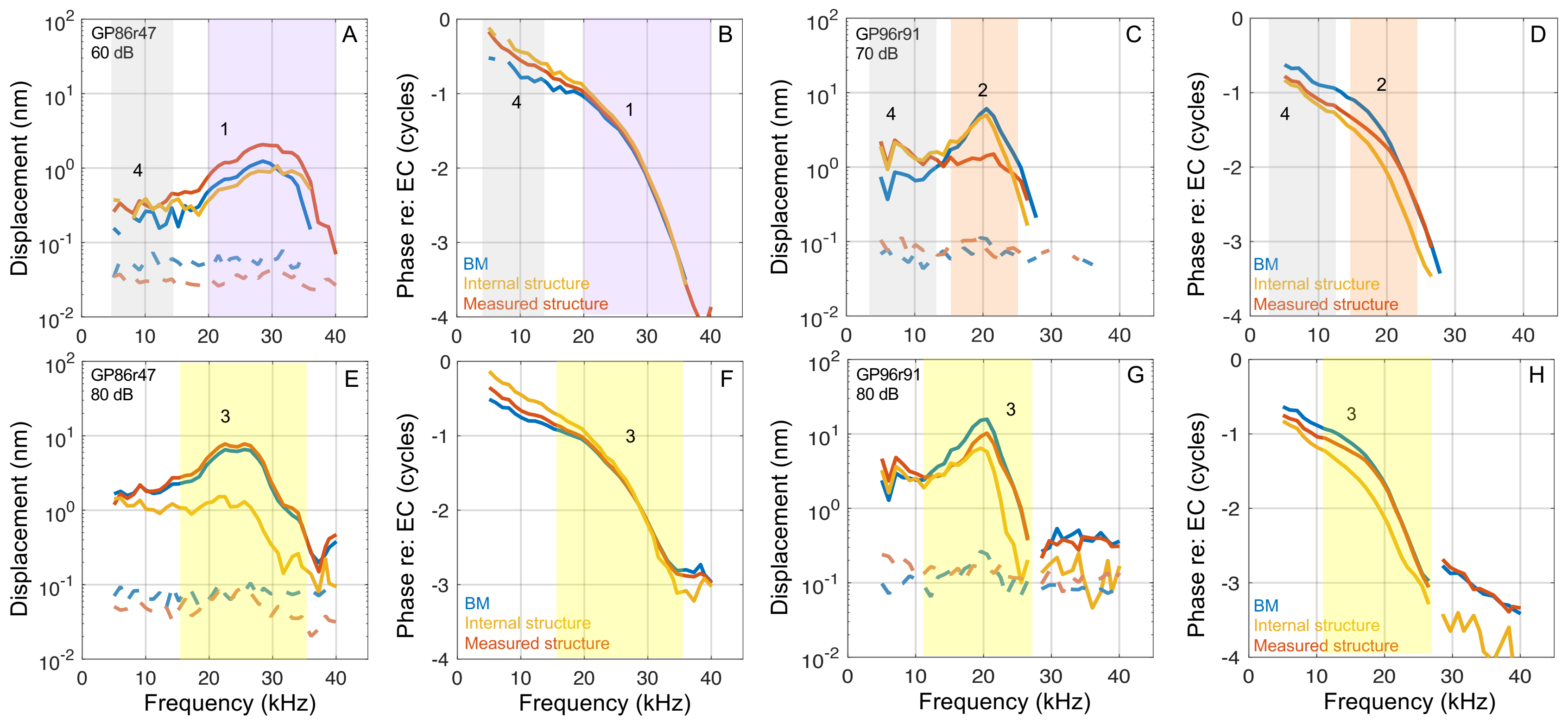

Figure 5: BM, internal, and measured motion displacement and phase from two different experiments (figures 3 & 4) showcasing different scenarios of relative motion between the structures. Internal motion analysis performed as described in methods, $\vec{X}_{int} = \vec{X}_{meas} - \vec{X}_{BM}$. Shaded regions with numbers correspond to the list to the left describing different relative relationships between BM and internal motion. (A-B) Complex difference analysis for GP86 Run 47 60 dB displacement (A) and phase (B). (C-D) Complex difference analysis for GP96 Run 91 70 dB displacement (C) and phase (D). (E-F) GP86 Run 47 80 dB displacement (E) and phase (F). (G-H) GP96 Run 91 80 dB displacement (G) and phase (H). E-F and G-H show different degrees of the third scenario. In E-F, internal motion is very small across frequencies, so the measured motion is most similar to that of the BM motion in magnitude and phase. On the other hand, in (G-H), the internal motion is larger, but still less than BM motion, resulting in a measured motion magnitude between internal and BM motion, and a shift in the measured motion phase from in phase with internal motion to in phase with BM motion.

Discussion

Reconstructed Tuning Curves – Internal Motion Details Visualized

- Plotting the internal motion at each SPL together forms "internal tuning curve"
- Fewer differences in phase across SPL
  - Lack of phase fan in GP86 run 47 at low frequencies
  - Lack of phase lift in GP96 run 91

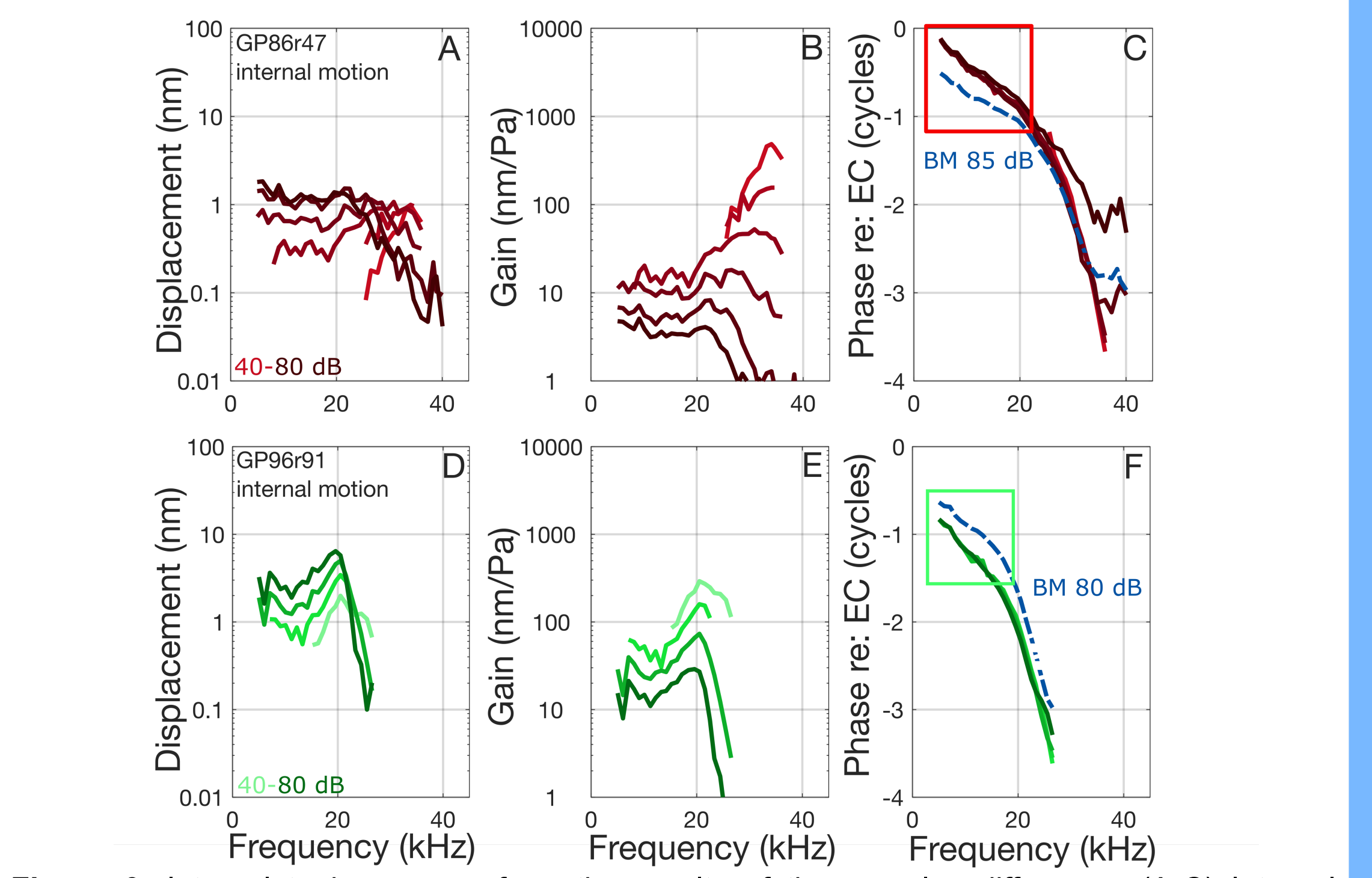

Figure 6: Internal tuning curves from the results of the complex difference. (A-C) Internal displacement, gain, and phase re: EC of GP86 run 47. 80 dB BM phase from Figure 3C also plotted in (C) for comparison. (D-F) Internal displacement (in nm), gain (in nm/Pa), and phase (in cycles re: ECP) of GP86 run 47. 80 dB BM phase also from Figure 4C also plotted in (F) for comparison.

- Evaluate gain ratio at $0.5 * BF$ to quantify degree of sub-BF nonlinearity *[1]*

$$GR = \frac{G_{0.5BF60}}{G_{0.5BF80}}$$

- Compare before and after complex difference calculation

	Measured	Internal
GP86 Run 47	1.58	3.5
GP96 Run 91	2.3	3.3

Table 1: Comparisons of gain ratio (GR) before and after complex difference analysis. Measured and internal GP86 run 47 GR calculated at $0.5 * BF = 17kHz$ in Figure 3F & 6B, respectively. GP96 run 91 measured and internal GR calculated at $0.5 * BF = 14kHz$ in Figure 4F & 6E, respectively.

- Sub-BF nonlinearity can be more prominent in internal motion than measured motion

Conclusions

Performing the complex difference analysis provides insight into the motion of internal structures in the reference frame of the BM. Depending on the sound pressure level, the relative amplitudes of BM motion and internal structure motion can vary across frequencies. When taking the motion of the structure directly from the OCT, what appears to be changes in the relative phase between structures could actually be the internal structure appearing to move with BM because the BM motion is much larger.

Frost et al. demonstrated the significance in knowing the optical coordinates relative to the anatomical coordinates of the cochlea *[5]*. Similarly, awareness of differences between the internal OC motion in the reference frame of the BM as opposed to directly output from the BM provides insight into the nuances of motion throughout the OC.

References

[1] Strimbu, C. E., Chiriboga, L. A., Frost, B. L., & Olson, E. S. (2024). Regional differences in cochlear nonlinearity across the basal organ of Corti of gerbil. Hearing Research, 443, 108951. https://doi.org/10.1016/j.heares.2024.108951

[2] Strimbu, C. E., Wang, Y., & Olson, E. S. (2020). Manipulation of the Endocochlear Potential Reveals Two Distinct Types of Cochlear Nonlinearity. Biophysical Journal, 119(10), 2087–2101. https://doi.org/10.1016/j.bpj.2020.10.005

[3] Fallah, E., Strimbu, C. E., & Olson, E. S. (2021). Nonlinearity of intracochlear motion and local cochlear microphonic: Comparison between guinea pig and gerbil. Hearing Research, 405, 108234. https://doi.org/10.1016/j.heares.2021.108234

[4] van der Heijden, M., & Joris, P. X. (2003). Cochlear Phase and Amplitude Retrieved from the Auditory Nerve at Arbitrary Frequencies. The Journal of Neuroscience, 23(27), 9194–9198. https://doi.org/10.1523/JNEUROSCI.23-27-09194.2003

[5] Frost, B. L., Strimbu, C. E., & Olson, E. S. (2022). Using volumetric optical coherence tomography to achieve spatially resolved organ of Corti vibration measurements. The Journal of the Acoustical Society of America, 151(2), 1115–1124. https://doi.org/10.1121/10.0009576

Acknowledgements

This work is supported by the NIDCD and the Emil Capita Foundation. We thank Kaitlyn Wong, Brian Frost, and Fowler Lab members past and present.